Polymersomes

DOI: 10.1002/ange.201300397

Breathing Polymersomes: CO_2-Tuning Membrane Permeability for Size-Selective Release, Separation, and Reaction**

*Qiang Yan, Jianbo Wang, Yingwu Yin, and Jinying Yuan**

Selective substance channels and confined reaction spaces that span scales ranging from the macroscopic world down to nanometer-sized structures are abundant in biological systems.[1] A basic entity is a cell, the membrane of which offers a confining boundary to control substance exchange and to compartmentalize complex biochemical processes. To comprehend the selective permeation mechanism of lipid membranes and to imitate their working principles, biomimetic cellular models have been explored.[2] Several artificial liposome systems with membrane selectivity have been successfully developed.[3] Within the last few years, a polymer-based equivalent, the polymersome, has come to be regarded as a promising candidate for such a system.[4] By tailoring the polymer structure and altering the polymer composition, one can endow these polymersomes with tunable permeability.[5] For example, Meier et al. studied the use of channel proteins and block copolymer bioconjugated membranes to selectively filter guest molecules.[6] Recently, an effective method based on the self-assembly of stimuli-responsive block copolymers was used to build intelligent vesicles.[7] This approach allows the bilayer gates to turn on and off when an external stimulus is given.[8] Herein, to enrich the scope of responsive polymersomes and improve polymeric membrane selectivity, we propose a new method to tune the permeability of polymersome membranes by means of carbon-dioxide-responsive copolymers. Utilizing CO_2 levels to control the size of nanopores in the membrane, these nanocontainers can attain the goal of releasing and separating globular nanoparticles of different sizes. Furthermore, they have the potential to act as nanoreactors that can insulate different catalytic reactions with the aid of CO_2-regulated transmembrane traffic.

We have synthesized a series of amphiphilic block copolymers, consisting of biocompatible and nonimmunogenic poly(ethylene glycol) (PEG) for the hydrophilic portion, and CO_2-sensitive poly(*N*-amidino)dodecyl acrylamide (PAD) as the hydrophobic portion. The target diblock copolymers, PEG-*b*-PAD, were prepared by atom transfer radical polymerization (Scheme 1 a).[9] Owing to their amphiphilicity, the copolymers can self-assemble into vesicular nanostructures in aqueous solution, and, most importantly, the polymersomes can continuously self-expand in a CO_2 atmosphere.[9] Once vesicular shape changes, the membrane structure and permeability must alter. On the basis of this concept, we wondered if we could make use of CO_2 as a stimulus to tune polymersome membrane permeability over a broad range.

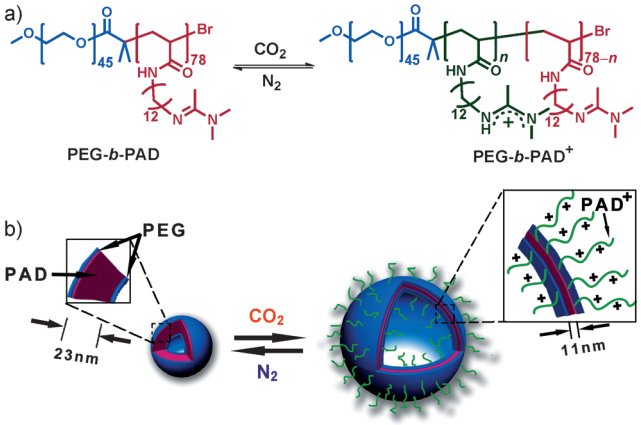

Scheme 1. a) Gas-switchable chemical structural change of the PEG-*b*-PAD block copolymer. b) The self-assembly of the copolymer into polymersomes and reversible gas-controlled breathing behavior in aqueous media.

We first tested the self-assembly behavior of the PEG-*b*-PAD in aqueous solution. The critical aggregation concentration (CAC) is ca. 0.12 mg mL^{-1} (Supporting Information, Figure S3). Transmission electron microscopy (TEM) showed that the average size of the initial vesicles was (112 ± 6.0) nm, which is consistent with the hydrodynamic radius (R_h) of 59.8 nm determined by dynamic light scattering (DLS; Figure 1 a and d) analysis. As expected, these vesicles started to expand when CO_2 passed through the solution at a rate of 1.0 mL min^{-1}. As shown in Figure 1 b, much larger intact vesicles with diameters of (151 ± 28) nm were found after 10 min of CO_2 treatment. Under these conditions, the R_h of these aggregates increased to 83.5 nm, which corresponds to the TEM results. When the CO_2 aeration time was prolonged to 30 min, the polymersomes finally extended to a maximum diameter of (238 ± 26) nm (Figure 1 c), which is close to the value of 137.2 nm determined by DLS analysis. The change in vesicle size is proportional to the gas stimulation time, and their radii grow at a constant rate of ca. 2.5 nm min^{-1}

[*] Dr. Q. Yan, Prof. Dr. Y. W. Yin, Prof. Dr. J. Y. Yuan
Key Lab of Organic Optoelectronics & Engineering Department of Chemistry, Tsinghua University, Beijing 100084 (P.R. China)
E-mail: yuanjy@mail.tsinghua.edu.cn
Prof. J. B. Wang
Computer Science School, China Women's University
Beijing 100084 (P.R. China)

[**] This work was financially supported by the National Basic Research Program (2009CB930602) and the National Natural Science Foundation of China (51073090 and 21174076). The authors acknowledge the help of J. X. Ma at the Beijing Chemical Research Centre with PEI compounds and enzyme-loaded experiments.
Supporting information for this article is available on the WWW under http://dx.doi.org/10.1002/anie.201300397.

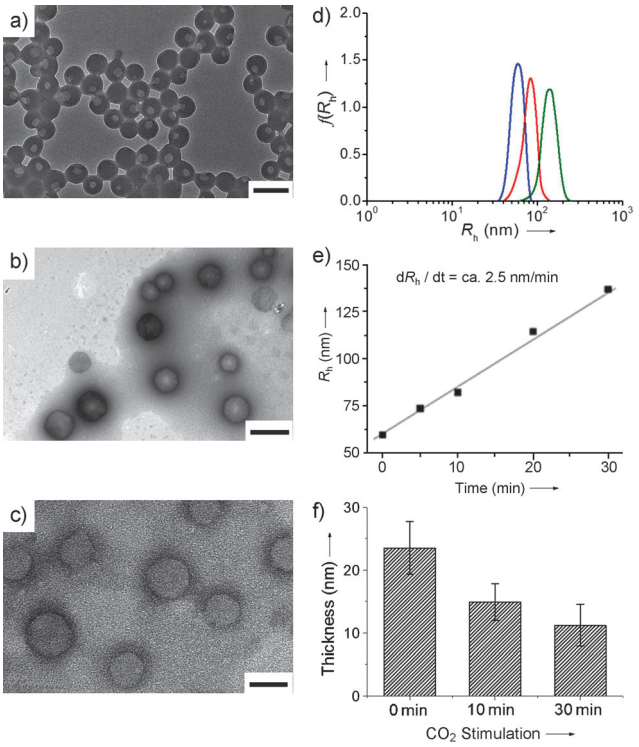

Figure 1. a)–c) TEM images showing the morphological changes in the PEG-*b*-PAD vesicles under different conditions; a) no stimulus, b) after 10 min of CO_2 exposure, c) after 30 min of CO_2 exposure; scale bars are 200 nm. d) DLS data for the size changes of the PEG-*b*-PAD vesicles; no stimulus (——), 10 min of CO_2 (——), and 30 min of CO_2 (——). e) The vesicle size growth rate as a function of gas stimulation time. f) Membrane thickness variation of the polymersomes upon CO_2 addition. The polymer concentration in all experiments was 0.20 mg mL^{-1}.

(Figure 1 e). Furthermore, the polymersomes undergo reversible swelling/collapsing when exposed to CO_2/N_2 in an alternating fashion (Supporting Information, Figure S4). This reversible expansion and contraction of the vesicles in response to gas exposure is in many ways reminiscent of a cell "breathing" process.[9,10]

We have shown that the self-expansion mechanism of PEG-*b*-PAD polymersomes is entirely attributed to the structural change of the PAD chains.[9] Driven by CO_2, part of the PAD chains in the vesicle wall transform from an unprotonated, entangled state (polyamidine form) to a protonated, stretched state (polyamidinium form) that is incorporated into new hydrophilic corona, whereas uncharged PAD species are still retained in the hydrophobic vesicle wall. The polymersomes are obliged to expand gradually, accompanied by a ca.50 % drop off in membrane thickness from 23.5 nm to 11.2 nm (Figure 1 f) to attain lower interfacial free energy. From the TEM images (Figure 1 a–c), we can see indirect evidence that the thickness of the hydrophobic vesicle wall (the dark layer) gradually decreases. A depiction of this gas-triggered vesicle breathing can be seen in Scheme 1 b.

We next focused on how to use CO_2 to adjust membrane permeability. To this end, two kinds of dye-decorated hyperbranched poly(ethylene imine) nanoparticles, one functionalized with a pyrene (PY) periphery (PEI-5, 5000 Da, ca. 4 nm) and the other with rhodamine B (RB) end-capping (PEI-25, 25 000 Da, ca. 10 nm), were loaded in these vesicles. These dye-labeled nanoparticles approximate proteins in molecular size and are more appropriate than conventional inorganic silica or gold analogues, thus they are ideal test molecules and can be used to test membrane-selective permeation by tracking their release.

The first experiment revealed that the size of the polymersome membrane channels depends upon CO_2 concentration. In the beginning, PEI-5 and PEI-25 were enclosed in the vesicles during the copolymer self-assembly process (see the Supporting Information), and unpackaged nanoparticles were dialyzed, as confirmed by negligible dye signals in the UV/Vis spectra. As the guest molecules leak out of the vesicles, we can obtain a release curve by measuring the variations in the dye spectra at fixed time intervals. The typical UV/Vis absorption of PEI-5 (PY) at λ_{max} is 335 nm and for PEI-25 (RB) at λ_{max} it is 554 nm. In the absence of gas, the curves (line I in Figure 2 a,b) satisfy a free-release model and

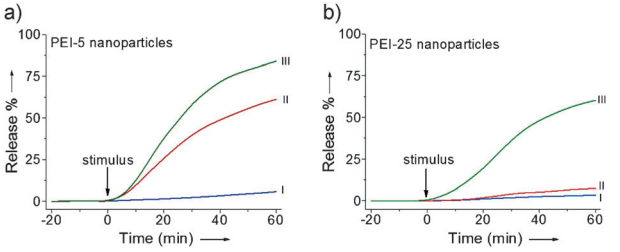

Figure 2. Release curves of PEG-*b*-PAD polymersomes loaded with PEI-5 nanoparticles (a) and PEI-25 nanoparticles (b) under different conditions; no stimulus (line I), 10 min of CO_2 (line II), and 30 min of CO_2 (line III). All guest-release experiments were carried out on a 1 h time scale.

the release quantities are less than 6 %. This suggests that both PEI-nanoparticles are too large to penetrate the compact vesicle membranes. However, after bubbling CO_2 through the solution for 10 min, the release rate of the smaller PEI-5 markedly increases and its release quantity reaches 61 % within 1 h. In contrast, the release of the larger PEI-25 was still inhibited (line II in Figure 2 a,b). That is to say, at the vesicles expansion stage the distensible membrane pores can allow the passage of PEI-5, but block PEI-25. After 30 min of CO_2 stimulation, both cargos show sharply increased liberation, with leakage ratios of 84 % and 62 % for PEI-5 and PEI-25, respectively (line III in Figure 2 a,b). The reason for this is that wall thickness drops to its lowest value, which leads to further amplification of membrane pore size, thus allowing the larger PEI-25 to escape. From these results, we deduced that CO_2 can effectively adjust the size of PEG-*b*-PAD polymersome membrane channels.

In view of the tunability of membrane permeation, it is anticipated that these vesicles could be further used as a miniature separator. For this purpose, equimolar amounts of PEI-5 and PEI-25, were enclosed together in nanocapsules (see the Supporting Information). To elucidate the selectivity of the membrane, CO_2-driven release experiments were performed (Figure 3 a). In step I, the nanoparticles displayed

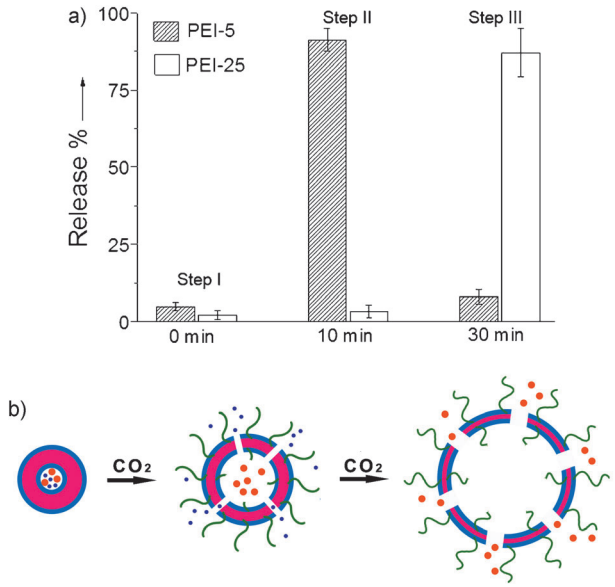

Figure 3. a) Separation differently sized nanoparticles (PEI-5 and PEI-25) by PEG-*b*-PAD vesicles; no stimulus and free release for 2 h (step I), 10 min of CO_2 stimulus and then incubation for 2 h (step II), an additional 30 min of CO_2 and then incubation for 2 h (step III); b) Illustration of the polymersomes acting as size-selective nanoseparators modulated by CO_2 levels.

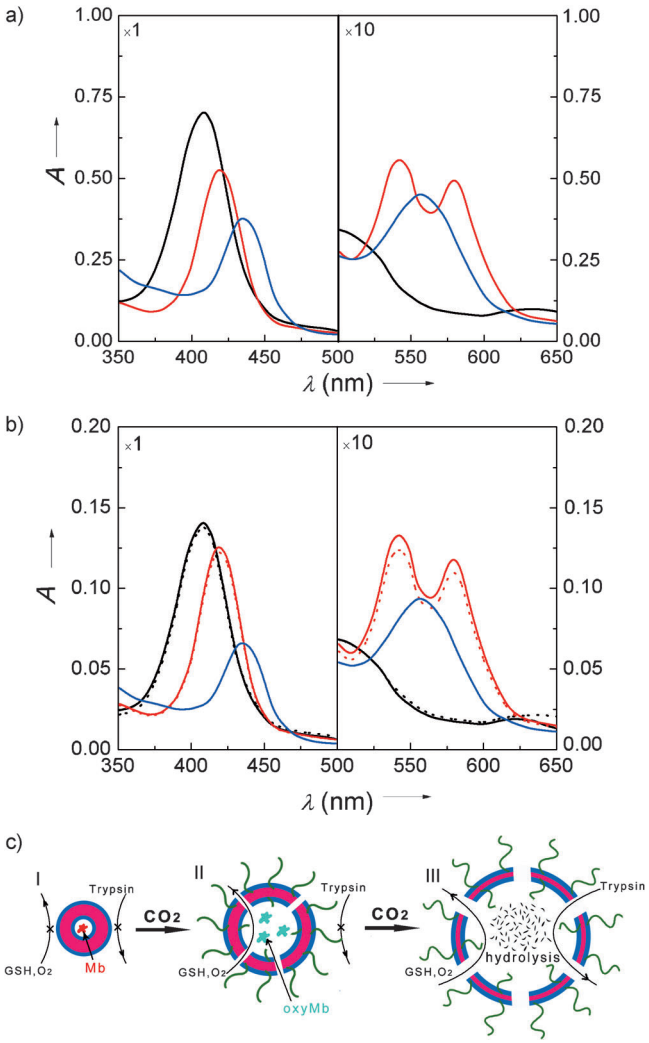

Figure 4. a) UV/Vis absorption spectra of free Mb solution (60 μg mL^{-1}) under different conditions; Mb (black line), after GSH reduction and further introduction of O_2 in the absence of trypsin (——), after incubation with trypsin (37 °C, 1 h, ——). b) UV/Vis absorption of Mb-loaded polymersomes (——) and under different conditions; introduction of GSH and O_2 (•••••), 5 min of CO_2 stimulation and then introduction of GSH and O_2 (——), incubation with trypsin (37 °C, 1 h, •••••), prolonging CO_2 stimulation for 15 min and then incubation with trypsin (37 °C, 1 h, ——); c) Illustration of the compartmentalization of two enzymatic reactions in the PEG-*b*-PAD polymersomes modulated by CO_2 levels.

free-release within 2 h in the absence of stimulation. Because the size of the inherent pores in the membrane (< 1.0 nm) is much smaller than that of nanoparticles, transmembrane transportation of both PEI-5 and PEI-25 is prohibited. In step II, after applying a short CO_2 stimulus (10 min) and then incubating the vesicle solution for the same time, 91 % of PEI-5 was observed to have leaked out, whereas the majority of PEI-25 was retained by the bilayers. The separation factor (α) between PEI-5 and PEI-25 is about 30.6, which is superior to the separation effect of chromatography. This high selectivity for PEI-5 indicates that the enlarged membrane pores nicely match the molecular size of PEI-5. In step III, the aeration time was extended to 30 min and the vesicles expanded to an extreme, resulting in high bilayer permeability. Hence, the remaining PEI-5 (8 %) and most of PEI-25 (87 %) escaped from the polymersomes. Actually, this process is equivalent to that of fractional extraction (Figure 3b). By means of step-controlled CO_2 levels, the overall separation selectivity of PEI-5 and PEI-25 is up to 96.8 % and 91.5 %, respectively. In a similar way, these CO_2-responsive vesicles have the potential to be used as selective nanoseparators to sieve complex mixtures of proteins based on their size differences.

Biochemical reaction compartmentalization is a crucial cellular characteristic. The tunable polymersome membrane stimulated us to create a synthetic nanoreactor that mimics enzymatic reaction compartments. Myoglobin (Mb), an iron-centered endogenous protein, was chosen as an enzyme model because its biological functions can be measured quantitatively by UV/Vis spectroscopy.[11] Normally, Mb displays a typical absorption at 409 nm, which corresponds to its Soret band (the black line in Figure 4a). The addition of glutathione (GSH) and then the introduction of O_2 to the solution induces a red shift of the Soret band to 419 nm, as well as a shape change in the Q band around 550 nm, which indicates the generation of O_2-carrying myoglobin (oxyMb, the red line in Figure 4a). Incubation of oxyMb in trypsin (a protease that can hydrolyze Mb) results in complete disappearance of the O_2-binding activity, as revealed by the new peak at 434 nm and the variation in the Q band around 550 nm (the blue line in Figure 4a). Because of the size difference between GSH and trypsin, we predicted that the vesicle membrane was likely to compartmentalize the enzymatic reactions. To verify this assumption, Mb was loaded into the PEG-*b*-PAD polymersomes. Unencapsulated Mb was removed from the Mb-loaded vesicles by centrifugation

(3 min at 12000 *g*) and the subsequent exchange of the supernatant with buffer solution (pH 7.4); this cycle was repeated five times. The suspension revealed a clear absorption at 409 nm, which was ascribed to the Mb, thus confirming successful encapsulation (the black line in Figure 4b). When we injected GSH and aerated the polymer solution with O_2, however, a UV/Vis absorption change was not observed within 1 h (the black dotted line in Figure 4b), which suggests that the initial small vesicles with low permeability hinder transmembrane transfer of GSH (Figure 4c, state I). However, when CO_2 gas was passed through the solution for 5 min beforehand to expand the vesicles, the spectrum rapidly showed a red shift (409→417 nm) and a double peak around 550 nm in the presence of GSH and O_2 (the red line in Figure 4b). It is attributed to the dilated membrane channels permitting GSH to travel through the bilayer to react with Mb. In contrast, although the larger vesicles generated at this stage allowed the membrane transport of small tripeptides, their permeability was not enough to permit the passage of bulky trypsin, as indicated by the lack of discernible spectroscopic changes, even when treated with trypsin for 1 h (the red dotted line in Figure 4b and state II in Figure 4c). Upon prolongation of the CO_2 stimulus to 15 min, the vesicles were further swollen and the channels further opened; as a result, the barrier to trypsin was broken. The new peak presented at 434 nm and the Q band around 550 nm vanished, which indicates that Mb has been completely hydrolyzed by trypsin (the blue line in Figure 4b). These results demonstrate that, through the control of CO_2 levels, these polymersomes can isolate two different enzymatic reactions (state III in Figure 4c).

In conclusion, we have successfully designed and developed a kind of biomimetic polymersome that can reversibly respond to CO_2, resulting in a distinctive breathing function. By regulating CO_2 stimulation time to induce the growth of these polymersomes, membrane permeability can be tuned. Utilizing this controlled semipermeability, we were able to realize hierarchical cargo release and the selective separation of guest molecules according to their size differences. Furthermore, the vesicle, like a cell, was shown to be capable of dividing different enzymatic catalytic reactions by simply modulating the CO_2 treatment levels. It is expected that these tunable polymersomes will allow researchers to better mimic cytomembranes and understand cellular functions.

Received: January 16, 2013
Published online: March 11, 2013

Keywords: biomimetic synthesis · carbon dioxide · membranes · nanostructures · polymers

[1] a) K. Renggli, P. Baumann, K. Langowska, O. Onaca, N. Bruns, W. Meier, *Adv. Funct. Mater.* **2011**, *21*, 1241 – 1259; b) D. M. Vriezema, M. C. Aragones, J. A. A. W. Elemans, J. J. L. M. Cornelissen, A. E. Rowan, R. J. M. Nolte, *Chem. Rev.* **2005**, *105*, 1445 – 1490.

[2] a) J. W. Szostak, D. P. Bartel, P. L. Luisi, *Nature* **2001**, *409*, 387 – 390; b) P. Tanner, P. Baumann, R. Enea, O. Onaca, C. Palivan, W. Meier, *Acc. Chem. Res.* **2011**, *44*, 1039 – 1049; c) R. Savic, L. B. Luo, A. Eisenberg, D. Maysinger, *Science* **2003**, *300*, 615 – 618; d) V. Noireaux, A. Libchaber, *Proc. Natl. Acad. Sci. USA* **2004**, *101*, 17669 – 17674; e) S. Belegrinou, J. Dorn, M. Kreiter, K. Kita-Tokarczyk, E.-K. Sinner, W. Meier, *Soft Matter* **2010**, *6*, 179 – 186.

[3] a) L. Petit, E. Maier, M. Gibert, M. R. Popoff, R. Benz, *J. Biol. Chem.* **2001**, *276*, 15736 – 15740; b) P. Jing, P. J. Rodgers, S. Amemiya, *J. Am. Chem. Soc.* **2009**, *131*, 2290 – 2296; c) D. Lee, J. N. Ashcraft, E. Verploegen, E. Pashkovski, D. A. Weitz, *Langmuir* **2009**, *25*, 5762 – 5766; d) S. Karve, G. B. Kempegowda, S. Sofou, *Langmuir* **2008**, *24*, 5679 – 5688; e) J. S. Hub, F. K. Winkler, M. Merrick, B. L. de Groot, *J. Am. Chem. Soc.* **2010**, *132*, 13251 – 13263; f) K. Niikura, K. Nambara, T. Okajima, Y. Matsuo, K. Ijiro, *Langmuir* **2010**, *26*, 9170 – 9175.

[4] a) J. C. M. van Hest, K. T. Kim, S. A. Meeuwissen, R. J. M. Nolte, *Nanoscale* **2010**, *2*, 844 – 858; b) S. F. M. van Dongen, H.-P. M. de Hoog, R. J. R. W. Peters, M. Nallani, R. J. M. Nolte, J. C. M. van Hest, *Chem. Rev.* **2009**, *109*, 6212 – 6274; c) C. G. Palivan, O. Fischer-Onanca, M. Delcea, F. Itel, W. Meier, *Chem. Soc. Rev.* **2012**, *41*, 2800 – 2823.

[5] a) J. Gaitzsch, D. Appelhans, L. Wang, G. Battaglia, B. Voit, *Angew. Chem.* **2012**, *124*, 4524 – 4527; *Angew. Chem. Int. Ed.* **2012**, *51*, 4448 – 4451; b) Z. K. Fu, M. Andreasson Ochsner, H.-P. M. de Hoog, N. Tomczak, M. Nallani, *Chem. Commun.* **2011**, *47*, 2862 – 2864; c) A. D. Price, A. N. Zelikin, Y. J. Wang, F. Caruso, *Angew. Chem.* **2009**, *121*, 335 – 338; *Angew. Chem. Int. Ed.* **2009**, *48*, 329 – 332; d) A. Kishimura, A. Koide, K. Osada, Y. Yamasaki, K. Katakoka, *Angew. Chem.* **2007**, *119*, 6197 – 6200; *Angew. Chem. Int. Ed.* **2007**, *46*, 6085 – 6088; e) G. Battaglia, A. J. Ryan, S. Tomas, *Langmuir* **2006**, *22*, 4910 – 4913; f) A. Carlsen, N. Glaser, J.-F. Le Meins, S. Lecommandoux, *Langmuir* **2011**, *27*, 4884 – 4890; g) R. Rodríguez-García, M. Mell, I. López-Montero, J. Netzel, T. Hellweg, F. Monroy, *Soft Matter* **2011**, *7*, 1532 – 1542.

[6] A. Ranquin, W. Verées, W. Meier, J. Steyaert, P. Van Gelder, *Nano Lett.* **2005**, *5*, 2220 – 2224.

[7] a) M. H. Li, P. Keller, *Soft Matter* **2009**, *5*, 927 – 937; b) O. Onaca, R. Enea, D. W. Hughes, W. Meier, *Macromol. Biosci.* **2009**, *9*, 129 – 139; c) Q. Yan, J. Y. Yuan, Z. N. Cai, Y. Xin, Y. Kang, Y. W. Yin, *J. Am. Chem. Soc.* **2010**, *132*, 9268 – 9270; d) R. J. Dong, B. S. Zhu, Y. F. Zhou, D. Y. Yan, X. Y. Zhu, *Angew. Chem.* **2012**, *124*, 11801 – 11805; *Angew. Chem. Int. Ed.* **2012**, *51*, 11633 – 11637; e) H. B. Jin, Y. L. Zheng, Y. Liu, H. X. Cheng, Y. F. Zhou, D. Y. Yan, *Angew. Chem.* **2011**, *123*, 10536 – 10540; *Angew. Chem. Int. Ed.* **2011**, *50*, 10352 – 10356; f) J. Z. Du, L. Fan, Q. M. Liu, *Macromolecules* **2012**, *45*, 8275 – 8283; g) D. H. Han, O. Biossiere, S. Kumar, X. Tong, L. Tremblaym, Y. Zhao, *Macromolecules* **2012**, *45*, 7440 – 7445; h) D. H. Han, X. Tong, O. Biossiere, Y. Zhao, *ACS Macro Lett.* **2012**, *1*, 57 – 61; i) B. Yan, D. H. Han, O. Boissiere, P. Ayotte, Y. Zhao, *Soft Matter* **2013**, *9*, 2011 – 2016.

[8] a) K. T. Kim, J. J. L. M. Cornelissen, R. J. M. Nolte, J. C. M. van Hest, *Adv. Mater.* **2009**, *21*, 2787 – 2791; b) S. F. M. van Dongen, W. P. R. Verdurmen, R. J. R. W. Peters, R. J. M. Nolte, R. Brock, J. C. M. van Hest, *Angew. Chem.* **2010**, *122*, 7371 – 7374; *Angew. Chem. Int. Ed.* **2010**, *49*, 7213 – 7216; c) A. Kishimura, S. Liamsuwan, H. Matsuda, W.-F. Dong, K. Osada, Y. Yamasaki, K. Kataoka, *Soft Matter* **2009**, *5*, 529 – 532.

[9] Q. Yan, R. Zhou, C. K. Fu, H. J. Zhang, Y. W. Yin, J. Y. Yuan, *Angew. Chem.* **2011**, *123*, 5025 – 5029; *Angew. Chem. Int. Ed.* **2011**, *50*, 4923 – 4927.

[10] S. Y. Yu, T. Azzam, I. Rouiller, A. Eisenberg, *J. Am. Chem. Soc.* **2009**, *131*, 10557 – 10566.

[11] I. Yamazaki, K. Yokota, K. Shikama, *J. Biol. Chem.* **1964**, *239*, 4151 – 4153.

